TN-65-21
A. W. Burfine
M. J. Lee

MAGNETIC FIELD MEASUREMENTS AND ENERGY CALIBRATION OF THE BEAM ANALYZING STATION SPECTROMETERS

I. INTRODUCTION

The energy spectrometer for the Beam Analyzing Stations[1] (BAS) consists of a bending magnet, a secondary emission spectrum monitor, and a beam dump. (see photo 1). To analyze the beam, the electrons are deflected upward by the magnet, passed through the spectrum monitor, and stopped by the dump. The spectrum monitor is a set of thin aluminum foils (see photo 2) situated in a plane which is perpendicular to the deflected beam axis and contains a focal point of the magnet.

The purpose of this note is to describe the two methods used for determining the location of a focal point, the foils' location, and the related energy calibration. One method is to find the magnet's effective length from field measurements and then calculate the location of the focal point theoretically for any desired energy calibration. The other method is to determine the focal point and energy calibration experimentally by the floating wire test. It has been found that both methods give the same result unless the wire required in the floating wire test is very long, e.g., greater than 25 feet.

II. FIELD MAPPING

Two 30°-30" magnets (see photo 1) of the same design[2] were procured for the Beam Analyzing Stations. The homogenity of the field of each magnet was

[1]Mechanical Design and Fabrication by E. Roskowski

[2]Design by H. Brechna

evaluated by field mapping. The mapping was done with a Hall-effect[3] gaussmeter which has an accuracy of 0.1%.[4] In the field measurement, the probe was set up perpendicular to the entrance mirror of the magnet on a long feed table moveable along z as shown in Fig.(1). A 6-inch cross feed was used for moving the probe across the pole face along x. A grid of points was taken at 1/2-inch intervals in the x-z plane. At $z = 16''$, a homogenity plot in the x direction was made. The values of the grid along each z were normalized to the value of the homogeneity plot in order to eliminate drift in the power supply and other equipment.

III. DETERMINATION OF MAGNET EFFECTIVE LENGTH

When a particle passes through a magnetic field, the particle energy, bending angle, and the field integral along the path are related by

$$\int \vec{B} \cdot d\vec{\ell} = \frac{\alpha E}{0.3} \text{ (kG, cm, MeV)} \tag{1}$$

The bending radius is given in units used by

$$\rho = \frac{E}{0.3 B} \tag{2}$$

The effective length ℓ of a magnet is defined to be the length of an ideal magnet which has the same bending angle α and maximum field B_o. Combining Eqs. (1) and (2), we find

$$\ell = \frac{1}{B_o} \int \vec{B} \cdot d\vec{\ell} \tag{3}$$

with the integration evaluated along an arc of radius ρ in the magnet.

---

[3]C. Germain," Bibliographical Review of the Methods of Measuring Magnetic Fields, Nuclear Instruments and Methods 21,"(1963), p. 17-46.

[4]F. W. Bell's Incremental Gaussmeter, Model 240.

From field measurements, the integral can be calculated along any path by interpolation.[5] The method of interpolation used for a calculation of the integral along an arc of radius 30" is described in Appendix I.

IV. DETERMINATION OF SPECTROMETER FOCAL POINT

A. Theoretical Method

With the magnet effective length known, a focal point of the spectrometer can be determined by calculation.[6] The coordinates of the focal point are given by

$$y' = P\,(1 - \cos\alpha) + t \sin\alpha \tag{4}$$

$$z' = y' \cot\alpha + \tan\frac{\alpha}{2} \tag{5}$$

where

$$t = \frac{P \cos(\alpha - \beta) \cos(\beta_1 + \beta_2)}{\cos\beta_1 (1 - \tan\beta_1 \tan\beta_2) \sin(\alpha - \beta_1 - \beta_2)} \tag{6}$$

and

t = distance between the focal point and the magnet exit pole face

β_1 = angle of rotation of entrance pole face

β_2 = angle of rotation of exit pole face.

1. Injector Phasing BAS spectrometer Focal Point Calculation

The maximum beam energy to be analyzed in the injector phasing BAS is 205 MeV. The physical size of the magnet is 30°-30". However, the effective length when measured along an arc of a 30" radius is 17.24" which corresponds to a 32.94°-30" magnet. The focal point will be calculated using the effective values.

[5] This computation was done on the B-5000 computer with a program written by S. K. Howry.

[6] Appendix II, Focal Point Calculation for a Bending Magnet

Consider finding the focal point for an energy calibration of 25 MeV/kG.[7] From Eq. (2) the corresponding bending radius is 32.8". With the physical orientation of the magnet as shown in Fig. (2), the following parameters can be determined from the geometry, viz., $\alpha = 30.0^\circ$, $\beta_1 = -1.47^\circ$, and $\beta_2 = -1.48^\circ$, assuming the effective pole faces were those of an ideal 32.94°-30" magnet.

Using Eqs. (4), (5) and (6), we find $y' = 30.3''$, $z_0' = 61.29''$ and $t_0' = 51.58''$, measured with respect to the effective point of entry O' for the central beam. With respect to the physical point of entry O the value of y' is essentially unchanged, but $z' \approx z_0' - \overline{OO'} = 60.52''$. The result and some of the design parameters are summarized in Table I.

2. Sector Test Station Focal Point Calculation

The maximum beam energy to be analyzed at the sector test station is 1.45 BeV. Limited by field saturation, the maximum usable field for the magnet is about 15 kG. This corresponds to an energy calibration of 96.7 MeV/kG and a bending radius of 126.9". The effective length of the magnet is 17.02" corresponding to a 32.51°-30" magnet. Figure (3) shows the physical orientation of the magnet which was chosen for equal maximum deviation of the central beam trajectory ($\rho = 126.9''$) from the geometric central axis.

From the geometry of the spectrometer, taking into account the effective magnet dimensions, the focal point was calculated. The result and some of the design parameters are given in Table I.

B. Experimental Method

Another method for finding a focal point and the related energy calibration is the floating wire test. This test requires no knowledge of the field distribution in the magnet.

---

[7] This was the energy calibration obtained experimentally by the floating wire test.

TABLE I

A SUMMARY OF PARAMETERS

for the

BAS SPECTROMETERS

	BAS Injector Phasing	BAS Sector Test
Maximum Energy	205 MeV	1450 MeV
Maximum Field	8 kG	15 kG
Maximum Current	120 amp	320 amp
Energy Calibration	25 MeV/kG	96.7 MeV/kG
Energy Acceptance	25%	25%
Bending Radius	32.9 inches	126.9 inches
Bending Angle	30°	7.7°
Pole Face Rotation:		
Entrance Face	-1.5°	-12.4°
Exit Face	-1.5°	-12.4°
Focal Point Location:		
Coordinates* — z' =	60.5 inches	230.9 inches
y' =	30.3 inches	30.2 inches
Distance from Exit Pole Face	51.6 inches	216.0 inches
Vacuum Pipe:		
Size — At Magnet Exit	1-3/4 inches	~ 2 inches
At Focal Plane	8-5/8 inches	8-5/8 inches

*Position is measured relative to the point of intersection of the magnet entrance pole face and the beam axis.

In the floating wire test, a beam of energy E is simulated by a current carrying wire which is under tension.[8] The relation is given by

$$E = 2.94 \frac{W}{I_W} \quad \text{(MeV, gm, Amp)} \tag{7}$$

where

W = wire tension

I_W = wire current

The experimental set-up for the floating wire test is shown in photo(3). The spectrum monitor foils are replaced by a wire attachment plate whose position from the magnet can be varied by sliding it along a 30° line. One end of an annealed wire[9] was rigidly attached to a point P on the sliding plate. The other end of the wire, (see photo 4) resting on a frictionless air-bearing pulley, was tied to a weighting pan with a mass of 10.046 grams located 48" from the magnet entrance pole face. The pulley was mounted on a table with an adjustable height, and the weighting pan was hung freely along its side. A precision scale S_1 was mounted 6" from the magnet entrance pole face and another scale S_2 was mounted 6" from the pulley. The magnet current I_m was fed by a 0-250 amp power supply with a current regulation of 1 part in 10^5. The wire current was obtained from a 0-1.5 amp power supply with a regulation of 1 part in 10^4. A set of precision weights ranging from 5 milligram to 100 gram was used to provide the proper wire tension. Initially, the sliding place was placed with P near its theoretical position (about 52" from the magnet exit pole face). For a uniform field magnet of this type, the loci of focal points

[8] Appendix III.

[9] Appendix IV, Some Experimental Considerations.

is approximately a straight line as shown in Fig. (4). Since P is constrained to move on such a line, the desired focal point F is the point of intersection of this line and the loci of focal points. The experimental goal was to adjust the parameters P, S_1, S_2, I_m, I_W, and W experimentally to determine F and the calibration of energy versus magnet current relative to F.

In the experiment, the height of the table was adjusted using a Paragon tilting level so that the pulley coincides with the beam axis. A convenient set of weights and wire current was selected to simulate an energy of approximately 250 MeV. The magnet current was adjusted for the wire to float in a position such that the wire crossed the scales S_1 and S_2 symmetrically ($S_1 = S_2$). This is a necessary condition because the wire had a slight catinary curve due to its finite mass. The table was moved either up or down, and with a telescope the corresponding δS_1 and δS_2 were measured.

If $\delta S_1 = \delta S_2$, then $P = F$;

if $\delta S_1 > \delta S_2$, P is too close to the magnet;

if $\delta S_1 < \delta S_2$, P is too far from the magnet.

These situations are depicted in Fig. (5). Subsequently, P was corrected accordingly, and the steps were repeated starting with the pulley at its initial position and adjusting the magnet current for wire symmetry, i.e., $S_1 = S_2$, Experimentally this procedure converged very rapidly as illustrated by the data given in Table II.

Having found F, energy versus magnet current was then determined. A set of weights and wire current was selected corresponding to a set of values of energy to be simulated. With the pulley at its initial position, the magnet current was adjusted for wire symmetry and the value was recorded. For completeness, the data of our experimental calibration are shown in Table III.

TABLE II

A SUMMARY OF THE FLOATING WIRE TEST DATA

(I_w = 0.5901 amp, w = 50.47 g)

I_m(amp)	δS_1(mils)	δS_2(mils)	Remarks
151.42	0	0	Starting
	+75	+80	Table was up
	-86	-94	Table was down
151.40	0	0	Moved P up 1/16"
	+85	+90	Table was up
	-86	-90	Table was down
151.28	0	0	Moved P up 1/16"
	+89	+89	Table was up
	-89	-89	Table was down
			P = F

The final location of P was found to be $y_o \sim 30"$ and $z_o \sim 60"$.

TABLE III

ENERGY CALIBRATION OF INJECTOR PHASING δS_2 SPECTROMETER

I_{wire} (Selected) amp	W (Selected) gm	I_{magnet} (Adjusted) amp	B_{max} (Measured) kG	U (Calculated)
0.5845	50.47	151.28	10.1	251.71
0.6391	50.47	138.74	9.28	232.71
0.6900	50.47	126.58	8.6	215.05
0.7534	50.47	115.47	7.85	196.95
0.8511	50.47	101.74	6.97	174.34
1.1675	50.47	73.62	5.1	127.09
0.9157	30.47	56.87	3.9	97.83
1.2876	30.47	39.97	2.8	69.57
1.4049	20.47	24.14	1.75	42.84
~1.740	10.47	9.70	~0.75	17.69
				Avg. 25.0 Mev/kG

V. RESULTS

A homogeneity plot of the field or the injector phasing BAS magnet is shown in Fig. (6). It can be seen that variation of the field is less than 0.1% over a radial distance of ±0.75 inches from the magnet central axis.

The saturation characteristics of both magnets are shown in Fig. (7). A field of about 15 kG can be obtained for a current of 300 Amps with a saturation of about 20%.

The effective length for the injector phasing BAS magnet is 17.24", and for the sector test BAS magnet is 17.02" measured along a 30" arc. The energy calibration for both stations is shown in Figs. (8) and (9), respectively. Some of the design parameters are summarized in Table I on page 5.

For the injector phasing BAS spectrometer, the focal points obtained theoretically and experimentally are:

$$y' = 30.3'' \qquad z' = 60.52'' \text{ (theoretical)}$$

$$y' = 30.0'' \qquad z' = 60'' \text{ (experimental)}$$

for 200 MeV/8 kG.

It can be seen that both of these points lie on the same 30° line where the point P is constrained to move. As expected, the experimental measured focal point is closer to the magnet than the theoretical focal point due to the finite mass of the wire which tends to bring the point of convergence closer to the magnet. Since the distance of the focal point from the magnet exit pole face is 52", the difference in the two focal points is about 1% of this distance. The accuracy in either method is about the same order for this case.

For the sector test BAS spectrometer, the focal point obtained theoretically is:

$$y' = 30.\%'' \qquad z' = 231.9'',$$

for 1.45 BeV/15 kG (300 Amps).

The floating wire test was not used in this case to find the focal point. Since the focal point is about 20 feet from the magnet, the error introduced by the mass and the stiffness of the wire is intolerable. (however, the value of the effective length was checked experimentally with a floating wire.) The accuracy of the theoretical method is limited by the approximations made in the first order theory for calculating the trajectory. The overall accuracy in this case is about ±2%.

VI. CONCLUSIONS

Two independent methods, one theoretical and one experimental, have been used to fing the focal point for a deflecting magnet. Both methods give comparable results. The experimental method has the advantage that no detail knowledge of the magnet field is required. However, the usefulness of the experimental method is limited in accuracy by the inherent error in the measurement if the finite mass and the stiffness of the wire are not considered. For a 10 foot wire, the accuracy is about ±1%. For a wire longer than 25 feet, theoretical method is more preferable.

VII. ACKNOWLEDGEMENT

The author, M. Lee, would like to thank E. Roskowski for his untiring efforts in the designing and engineering of the beam analyzing stations, especially for those many night he spent in doint the floating wire tests, and the mechanical alignment and fabrication of the spectrometers.

APPENDIX I

NUMERICAL CALCULATIONS OF MAGNET FIELD PARAMETERS

The $\int \vec{B}.d\vec{\ell}$ of the Beam Analyzing Station bending magnet was approximated by interpolating points along the magnet central axis with the radius of curvature $\rho = 30''$. The method used for the multivariate interpolation was of separate interpolation of each of the independent variables. Since B is a function x and z, and x and z are equally spaced, we can tabulate B into a bivariate table.[10] A sample structure is shown:

Bivariate Table

$B(x_o, z_o)$	$B(x_o, z_1)$	. . .	$B(x_o, z_n)$	. . .
$B(x_1, Z_o)$	$B(x_1, z_1)$	. . .	$B(x_1, z_n)$	. . .
.	.	. . .	.	. . .
.	.	. . .	.	. . .
.	.	. . .	.	. . .
$B(x_m, z_o)$	$B(x_m, z_1)$	. . .	$B(x_m, z_n)$	. . .

Let

$$u = \frac{x - x_o}{h}$$

$$v = \frac{z - z_o}{h}$$

where

$$h = \Delta z = \Delta x \ .$$

The forward difference of B may now be tabulated in terms of u_n and v_n, both integers. From this table, b at any point can be found by using

[10] Kaiser S. Kunz, Numerical Analysis, McGraw-Hill, New York, p. 248 (1957)

the Gregory-Newton forward interpolation formula.[11]

$$B = B_o + u^{(1)} \Delta B_o + \frac{1}{2!} u^{(2)} \Delta^2 B_o + \ldots + \frac{1}{m!} u^{(m)} \Delta^m B_o$$

where

$$u^{(k)} = u(u - 1)(u - 2) \ldots (u - k + 1)$$

$$\Delta^n = n \text{ th forward difference}$$

The calculated value of $B(u,v)$ along S are then tabulated and $\int B d\ell$ can be found by numerical integration by using the Lorentz diagram:[12]

$$\frac{1}{h} \int_{\varphi_o}^{\varphi_o+h} B(\varphi)\, d\varphi = \frac{\Delta}{\ell n\ (1 + \Delta)} B_o \quad .$$

[11]Ibid, p. 54

[12]Ibid, p. 151

APPENDIX II

FOCAL POINT CALCULATION FOR A UNIFORM FIELD BENDING MAGNET

The field intensity, bending radius and the particle energy are related by[13]

$$B\rho \approx \frac{10}{3} E \text{ (kG, cm, MeV)}$$

where

B = magnetic field strength

ρ = bending radius, and

E = particle energy.

Let E_o be the energy of the central trajectory beam. Consider a particle with its energy given by $E = E_o + \Delta E$. If ΔE is small compared with E_o, the trajectory of the particle after passing through a uniform field magnet is given by:[14]

$$\begin{bmatrix} x \\ \theta \\ \frac{\Delta E}{E_o} \end{bmatrix} = \begin{bmatrix} \frac{\cos(\alpha-\beta_1)}{\cos\beta_1} & \rho \sin\alpha & \rho(1-\cos\alpha) \\ \frac{-(1-\tan\beta_1 \tan\beta_2)\sin(\alpha-\beta_1-\beta_2)}{\rho\cos(\beta_1+\beta_2)} & \frac{\cos(\alpha-\beta_2)}{\cos\beta_2} & \sin\alpha+(1-\cos\alpha)\tan\beta_2 \\ 0 & 0 & 1 \end{bmatrix} \cdot \begin{bmatrix} x_o \\ \theta_o \\ \frac{\Delta E}{E_o} \end{bmatrix} \quad (1)$$

where (x,θ) and (x_o,θ_o) are the position and angular coordinates and β_1 and β_2 are the pole face rotations measured relative to the central trajectory as shown in Fig. 6.

---

[13] John J. Livingood, Principles of Cyclic Particle Accelerators, p. 20

[14] S. Penner, "Calculations of Properties of Magnetic Deflection Systems," Rev. Sci. Instr. 32, p. 153.

Focal Point for Energy E_o With Normal Incidence and Exit

For the case with normal incidence and exit and $\Delta = = 0$, Eq. (2) reduces to

$$\begin{bmatrix} x \\ \theta \end{bmatrix} = \begin{bmatrix} \cos\alpha & \rho_o \sin\alpha \\ \frac{-\sin\alpha_o}{\rho_o} & \cos\alpha_o \end{bmatrix} \begin{bmatrix} x_o \\ \theta_o \end{bmatrix}, \tag{2}$$

The coordinates (x',θ') in any plane at a distance t from the magnet exit are related to (x,θ) by

$$\begin{bmatrix} x' \\ \theta' \end{bmatrix} = \begin{bmatrix} 1 & t \\ 0 & 1 \end{bmatrix} \begin{bmatrix} x \\ \theta \end{bmatrix}; \tag{3}$$

hence,

$$\begin{bmatrix} x \\ \theta' \end{bmatrix} = \begin{bmatrix} \left(\cos\alpha_o - \frac{t\sin\alpha_o}{\rho_o}\right) & (\rho\sin\alpha_o + t\cos\alpha_o) \\ -\frac{\sin\alpha_o}{\rho_o} & \cos\alpha_o \end{bmatrix} \begin{bmatrix} x_o \\ \theta_o \end{bmatrix} \tag{4}$$

By definition, the focal plane is a plane on which $x' = 0$ for the $\theta_o = 0$. Then it follows from Eq. (4) that for the focal plane

$$t = \rho_o \cot\alpha_o \ . \tag{5}$$

Let the coordinates of the focal point by (z'_o, y'_o) as shown in Fig. (10). It can be seen from the geometry of the system that

$$y'_o = \left(\frac{\rho_o}{\cos\alpha_o} - \rho_o\right)\cos\alpha_o + t\sin\alpha_o = \rho_o \tag{6}$$

and

$$z'_o = y'_o \cot \alpha + \rho_o \tan \frac{\alpha_o}{2} = \rho_o \left(\cot \alpha_o + \tan \frac{\alpha_o}{2}\right) \tag{7}$$

<u>Focal Point for Energy E_o With Arbitrary Incident and Exit Angles</u>

By repeating the same steps as those given in the previous section with β_1 and β_2 non-zero, we obtain

$$t = \frac{\rho \cos (\alpha - \beta_1 \cos (\beta_1 + \beta_2)}{\cos \beta_1 (1 - \tan \beta_1 \tan \beta_2) \sin (\alpha - \beta_1 - \beta_2)} \tag{8}$$

$$y' = \rho\ (1 - \cos \alpha) + t \sin \alpha \tag{9}$$

and

$$z' = y' \cot \alpha + \rho \tan \frac{\alpha}{2} \quad . \tag{10}$$

The angle β_1 or β_2 is positive for increasing focusing, i.e., moving the focal point closer to the magnet. In particular, when $\beta_1 = \beta_2 = \beta$,

$$t = \frac{\rho \cos (\alpha - \beta) \cos \beta}{\sin (\alpha - 2\beta)} \tag{11}$$

<u>Focal Point for Any Energy E With Normal Incidence</u>

In the spectrometer operation, the magnetic field B is adjusted so that particles with $E \simeq E_o$ will go through the focal point (y'_o, z'_o) at the center of a foil. The trajectory for particles with energy E_o has been previously analyzed. But the result of the analysis is also applicable for any E. As an example consider finding the focal point of a beam with energy $E < E_o$. Let

$$E = E_o + \Delta E$$

and (12)

$$\rho = \rho_o + \Delta\rho$$

If

$$\Delta E < 0$$

then

$$\Delta\rho = \frac{\Delta E}{E}\,\rho_o < 0 \; . \tag{13}$$

Figure (11) shows a diagram of the situation being considered. From the figure it may be seen that a particle with momentum $E < E_o$ will be deflected through an angle $\alpha > \alpha_o$. In addition, the exit pole face is rotated by an angle β_2, given by

$$\frac{\rho}{\sin \alpha_o} = \frac{-\Delta\rho}{\sin \beta_2} \tag{14}$$

Also

$$\alpha = \alpha_0 + \beta_2 \tag{15}$$

From the results of the previous section with $\beta_1 = 0$, we have

$$y' = \rho \left(1 + \frac{\cos \alpha \tan \beta_2}{\tan \alpha - \tan \beta_2} \right) \tag{16}$$

and

$$z' = \rho \left[\cot \alpha \left(1 + \frac{\cos \alpha \tan \beta_2}{\tan \alpha - \tan \beta_2} \right) + \tan \frac{\alpha}{2} \right] \tag{17}$$

where $\beta_2 > 0$ if $\Delta E < 0$ and $\beta_2 < 0$ if $\Delta E > 0$.

The loci of the focal points for a 30^o-30" magnet with $E_o = 200$ MeV have been calculated using these equations. The result is shown in Fig. (4).

APPENDIX III

FLOATING WIRE TEST

Consider the forces acting on a wire segment of length $d\ell$ as shown in Fig. (12). The force due to the magnetic field is given by $BI_W d\ell$ normal to the segment. At equilibrium, this force is balanced by the wire-tension:

$$2W \sin\left(\frac{d\theta}{2}\right) = BI_W d\ell \tag{1}$$

From Eq. (1), we obtain the equation for a wire carrying a current in a magnetic field:

$$\rho_W = \left(\frac{d\ell}{d\theta}\right) = \frac{W}{BI_W} \tag{2}$$

where ρ_W is the radius of curvature of the wire.

The equation for a charged particle in a magnetic field is given by:

$$BeV = \frac{mV^2}{\rho} \quad ,$$

or

$$\rho \cong \frac{E}{Bce} \tag{3}$$

for a highly relativistic particle. Thus, a beam of changed particles of energy E can be simulated by a floating wire if the particle trajectory coincides with the wire, i.e., the same radius of curvature for both:

$$E = ce\left(\frac{W}{I_W}\right) = 2.94\left(\frac{W}{I_W}\right) \text{(MeV, gm, amp)}. \tag{4}$$

To find a focal point, it is necessary to simulate a converging(parallel-incident) beam by the wire. For a given magnetic field, the wire must be floated such that it is parallel to the beam axis before the magnet while being held to a fixed point on the other side of the magnet. This fixed point is the focal point. Then by measuring the ratio of the wire-tension to wire-current, the corresponding energy can be determined from Eq. (4).

APPENDIX IV

SOME EXPERIMENTAL CONSIDERATIONS

The wire used for the experiment was 0.005-inch (No. 37) wire with a density of 1 mg per centimeter. The tension in the wire was provided by a 10.470 gram weight pan and a set of weights ranging from 10 mg to 100 grams, suspended from a pulley. The pulley was specially made with air bearings.

The wire current was supplied by an 18-volt, 1.5 amp current-regulated power supply. The wire current monitor was a 1 ohm, 0.05% watt resistor. The voltage across the resistor was measured on a 2401B Dymec Ingegrating Digital Voltmeter with a one-second gate. A K paragon tilting level was used to measure the deviation of the wire from parallel at several points.

A variable transformer was used to anneal the wire. With the wire stretched over the path, the wire was heated for about 10-15 minutes at 75 volts ac after which it was allowed to cool. The carbonized teflon coating on the wire was then washed off with acetone.

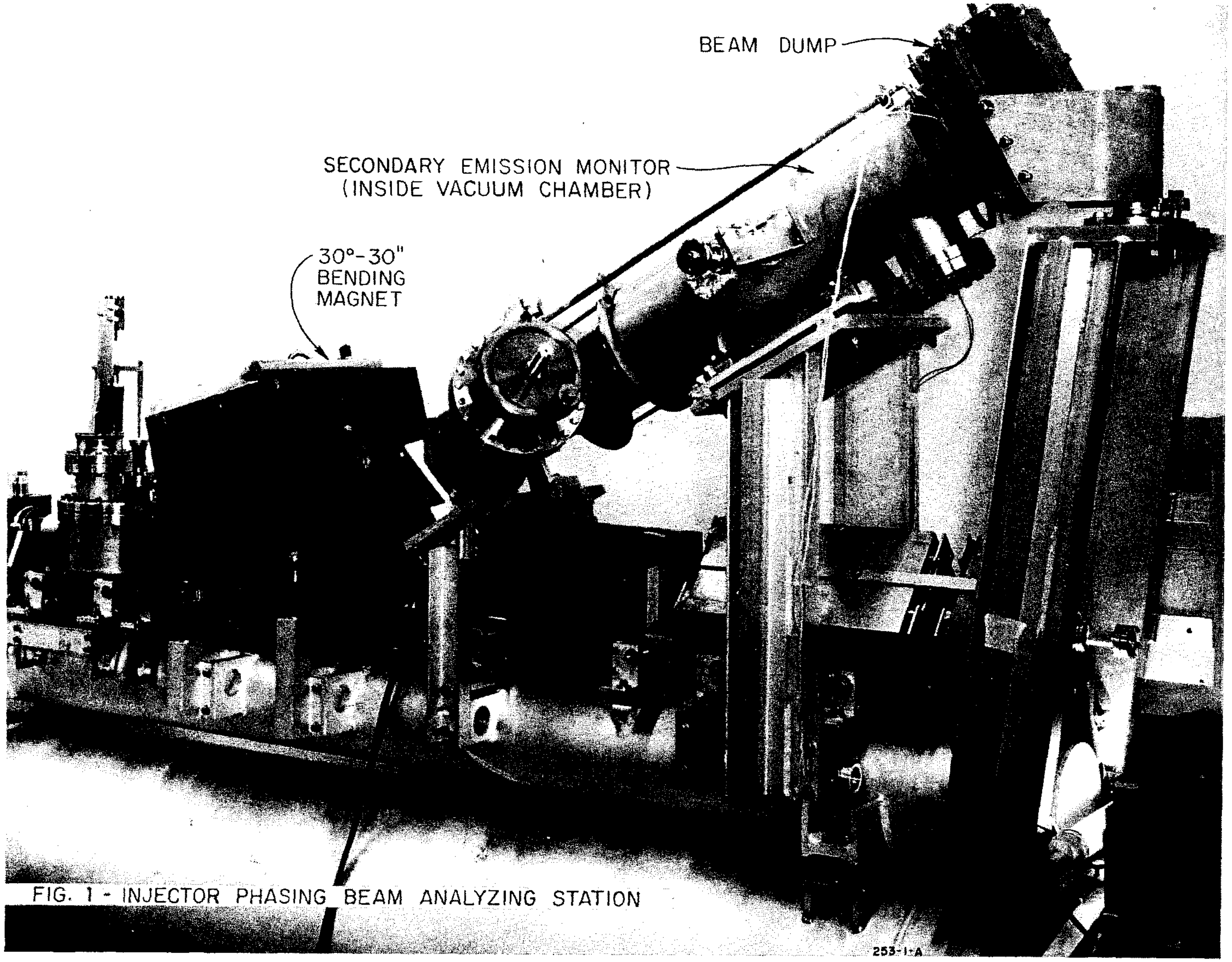

FIG. 1 - INJECTOR PHASING BEAM ANALYZING STATION

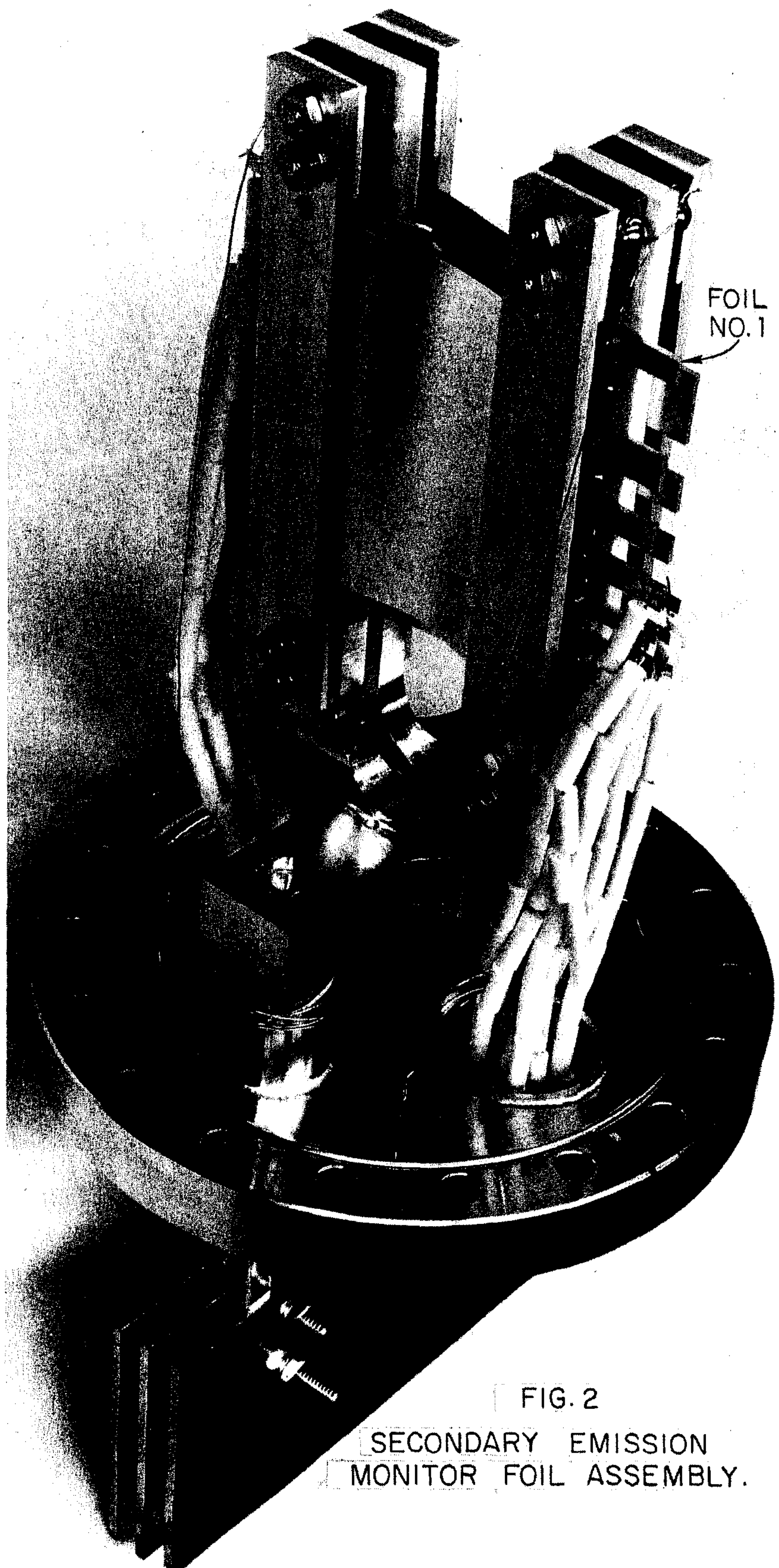

FIG. 2
SECONDARY EMISSION
MONITOR FOIL ASSEMBLY.

253-4-A

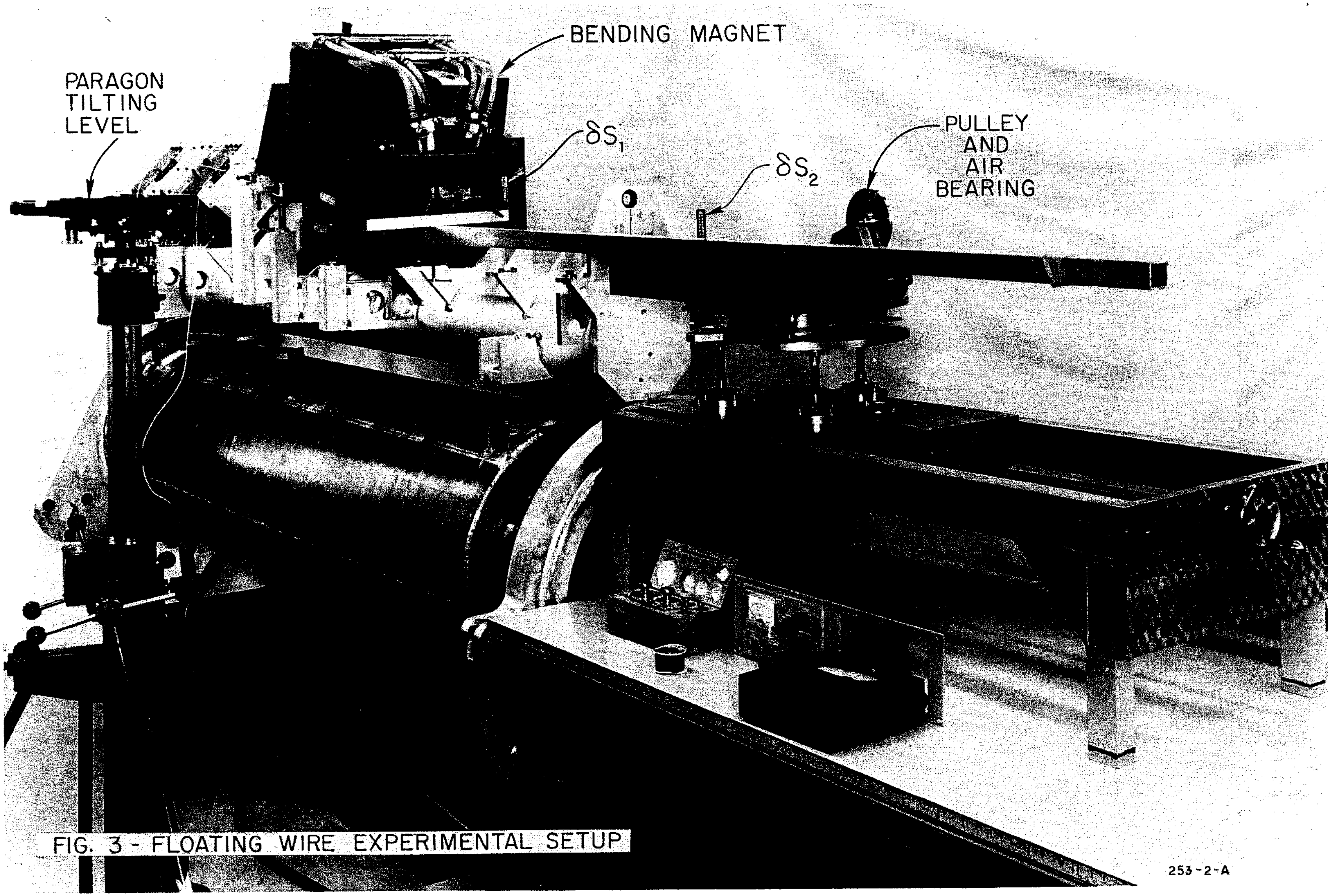

FIG. 3 - FLOATING WIRE EXPERIMENTAL SETUP

253-2-A

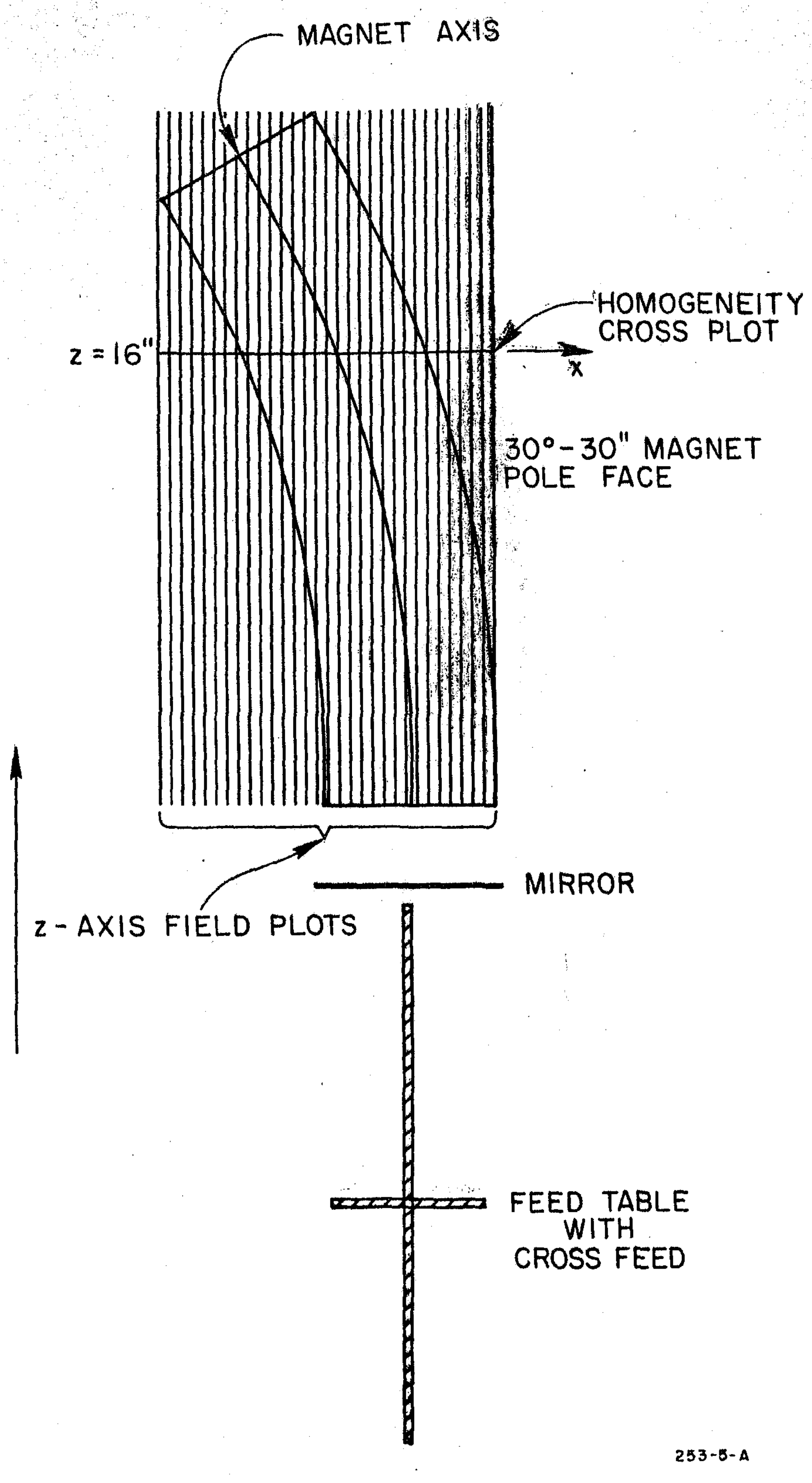

FIG. 4 - FIELD MAP GRID AND SETUP

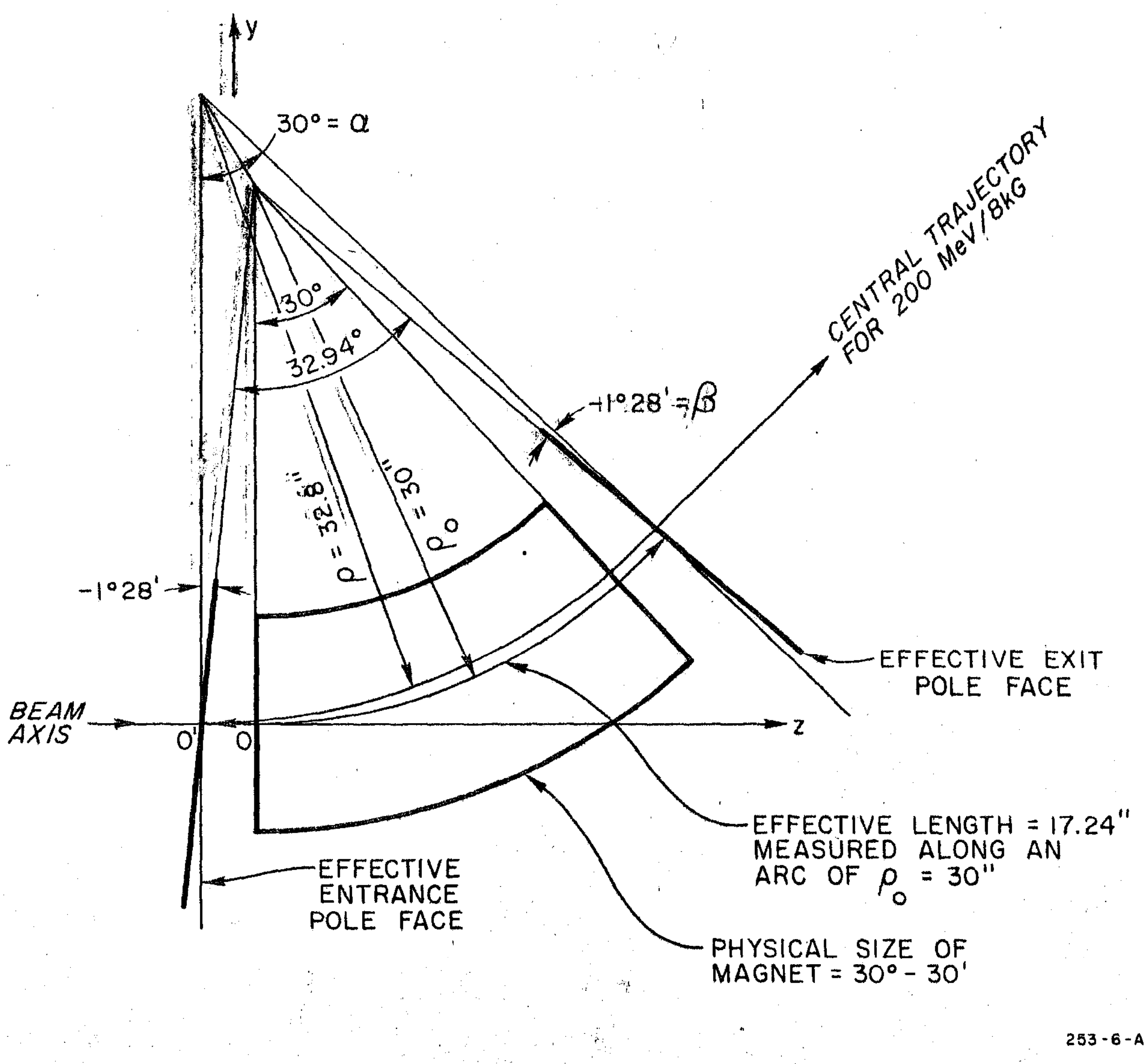

FIG. 5 - PHYSICAL ORIENTATION OF INJECTOR PHASING BAS SPECTROMETER

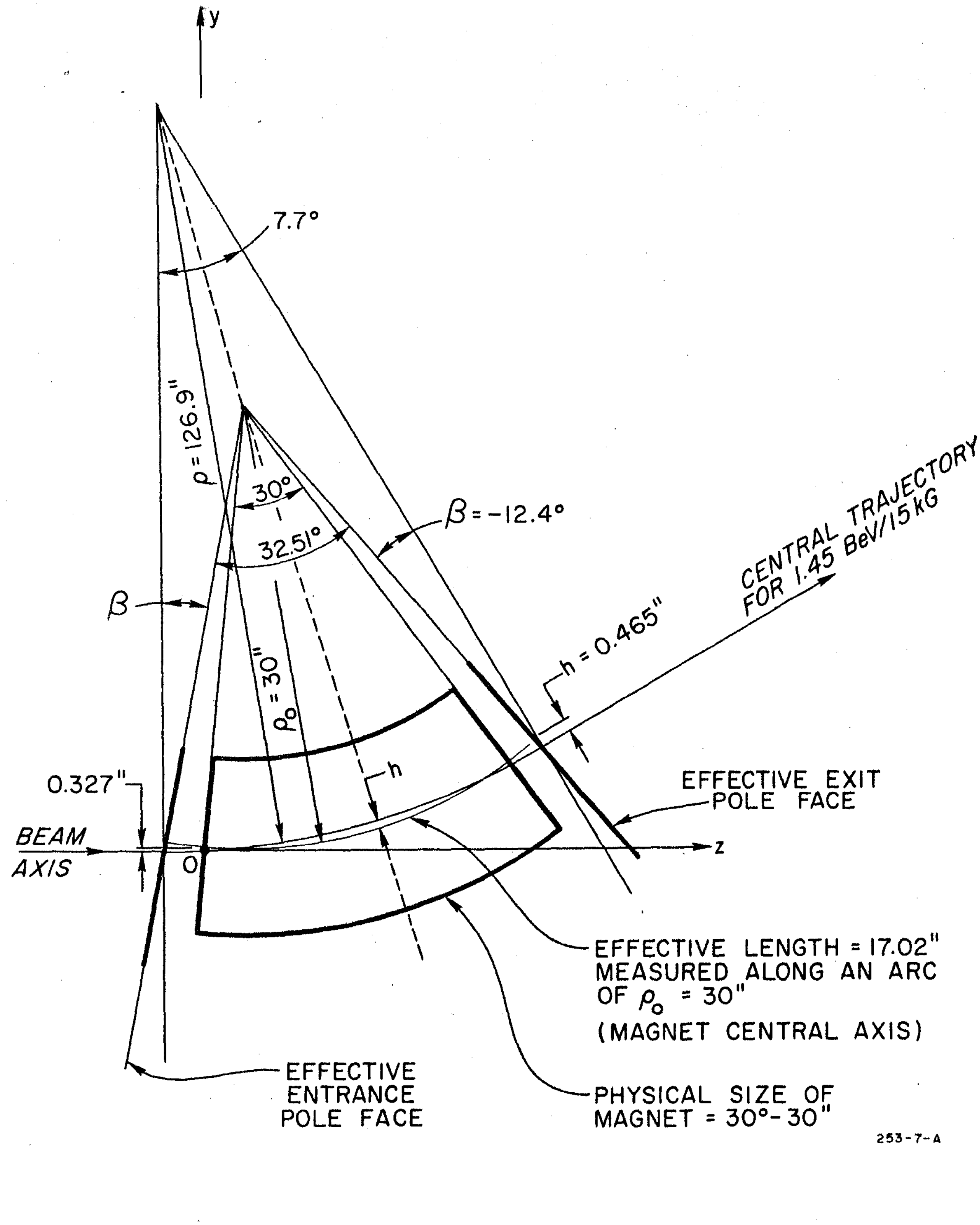

FIG. 6 - PHYSICAL ORIENTATION OF SECTOR TEST BAS SPECTROMETER

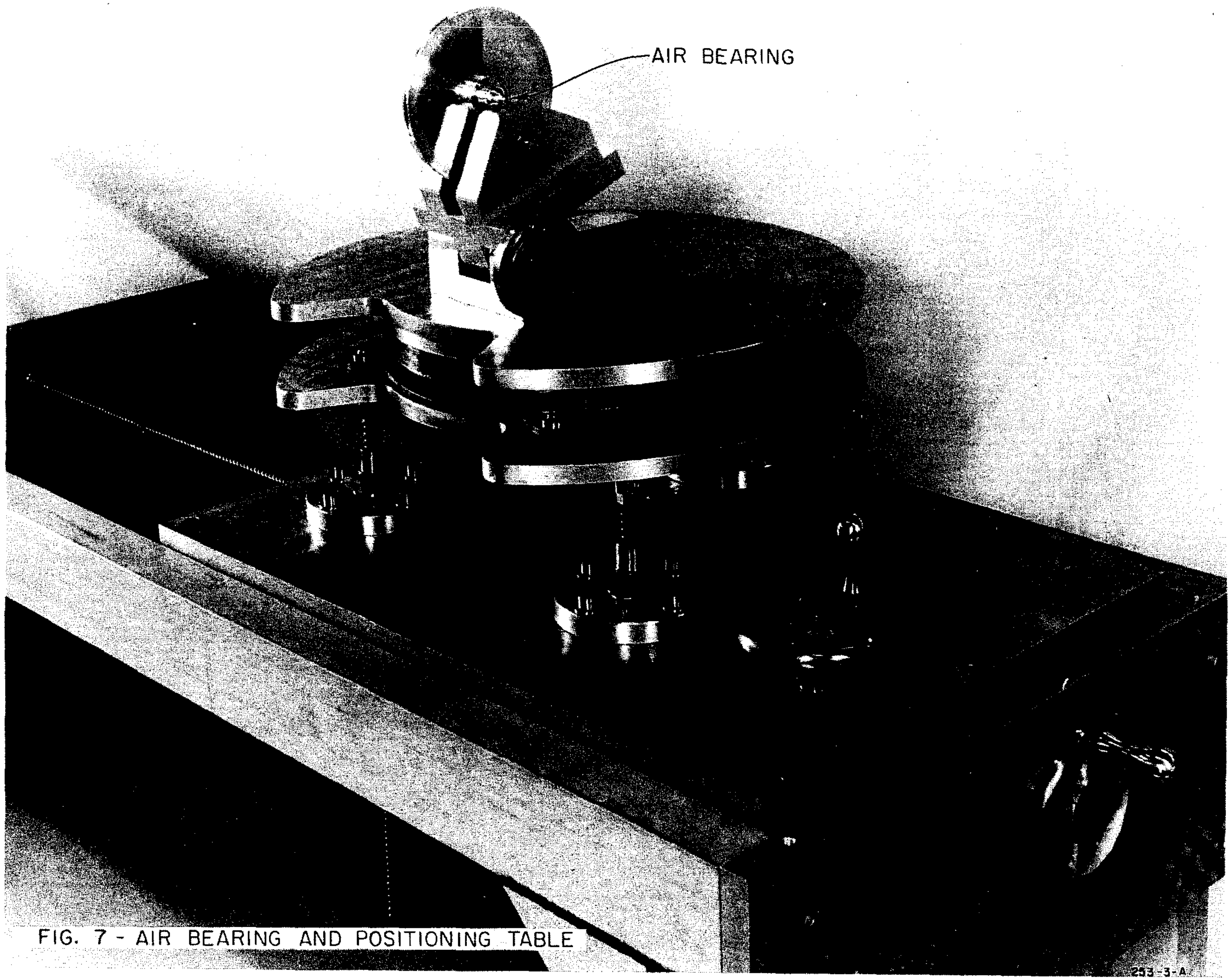

FIG. 7 - AIR BEARING AND POSITIONING TABLE

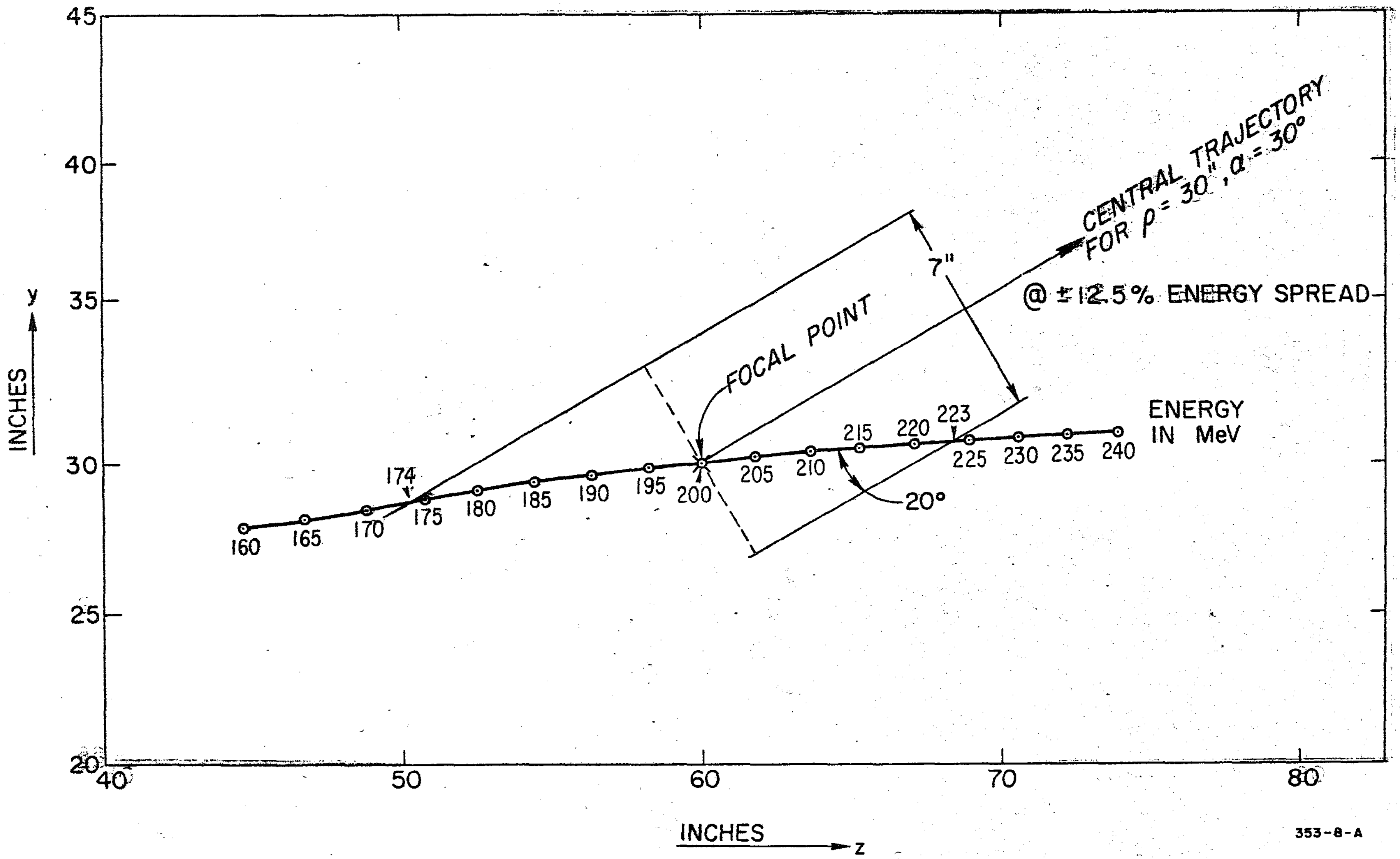

FIG. 8 - LOCI OF THE FOCAL POINTS FOR DIFFERENT BEAM ENERGIES FOR A 30°-30" DEFLECTING MAGNET (NORMAL INCIDENT CASE)

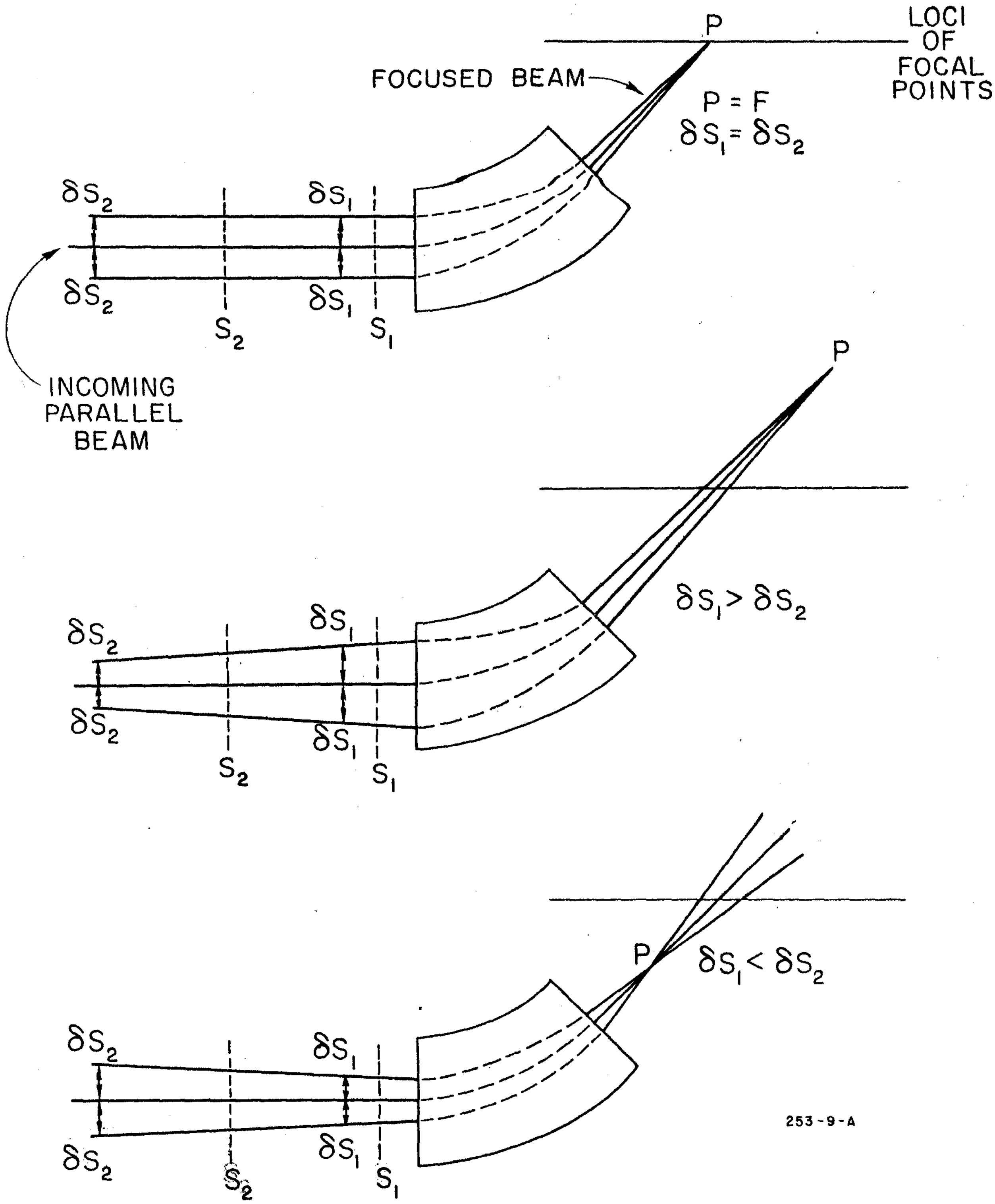

FIG. 9 - FLOATING WIRE FOR VARIOUS LOCATIONS OF P.

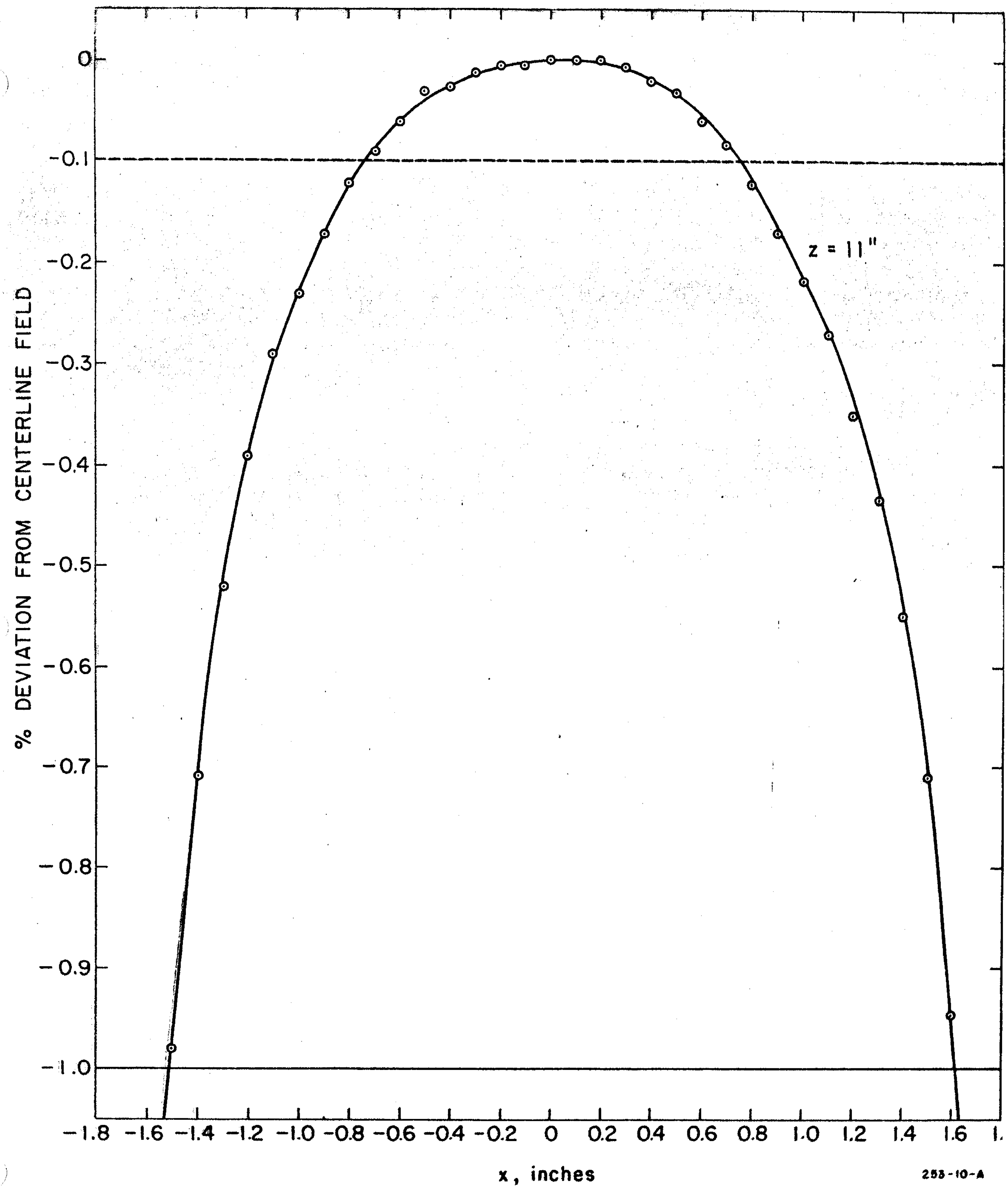

FIG. 10 - HOMOGENEITY OF INJECTOR PHASING BAS SPECTROMETER.

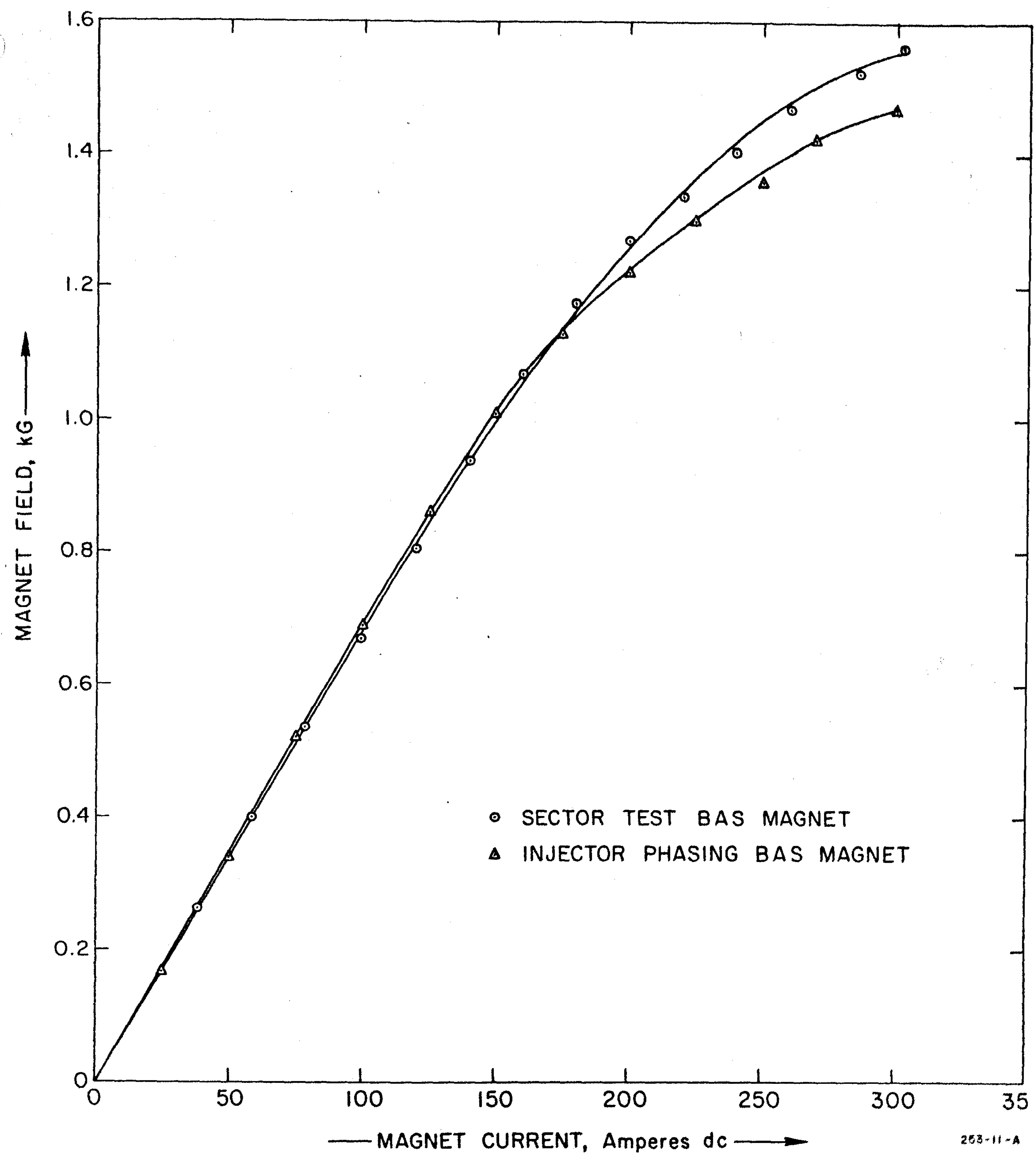

FIG. 11 - MAGNET SATURATION CHARACTERISTICS

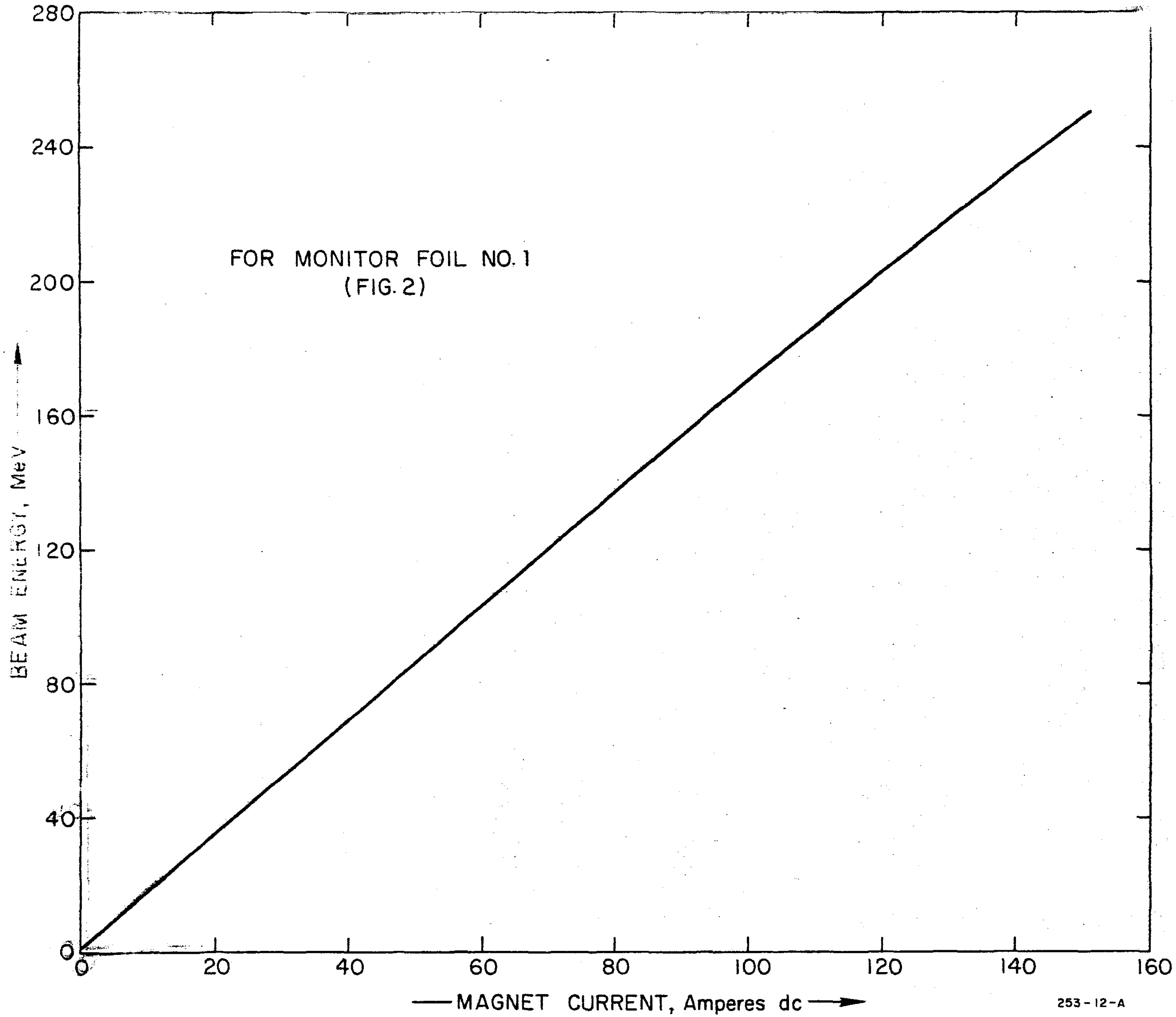

Fig. 12 ENERGY CALIBRATION INJECTOR PHASING RAS SPECTROMETER

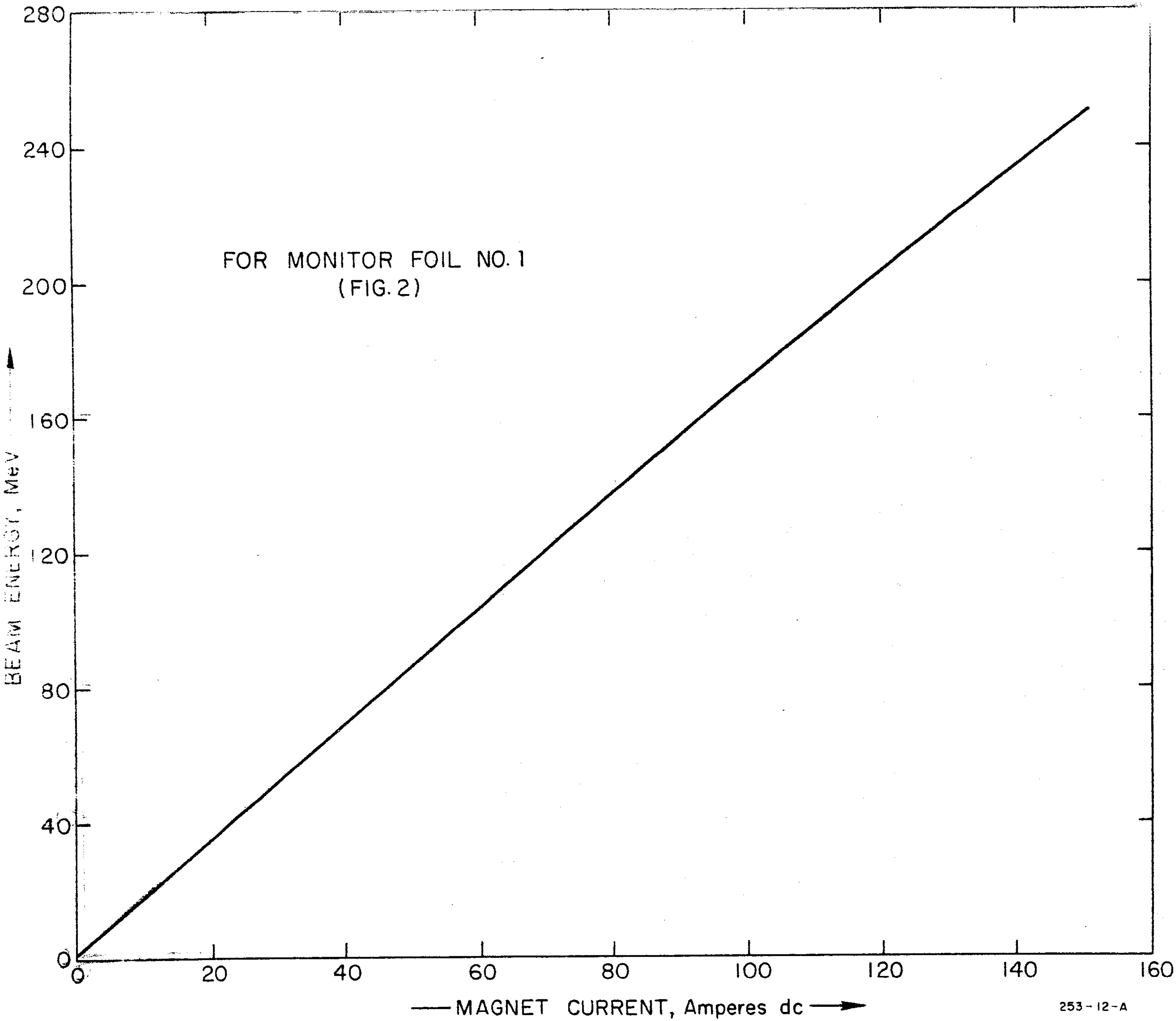

FIG. 12 - ENERGY CALIBRATION INJECTOR PHASING BAS SPECTROMETER

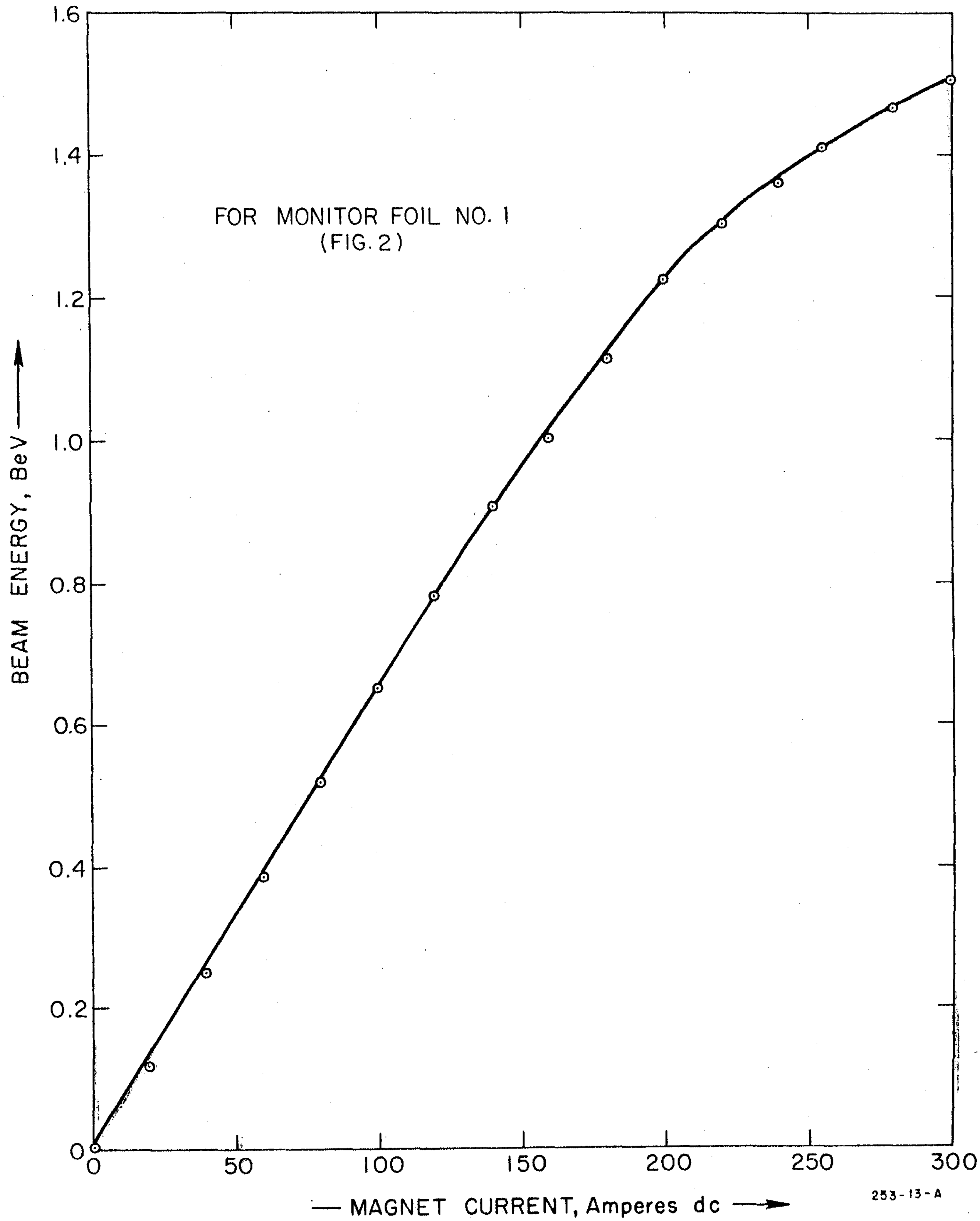

FIG. 13 - ENERGY CALIBRATION SECTOR TEST BAS SPECTROMETER.

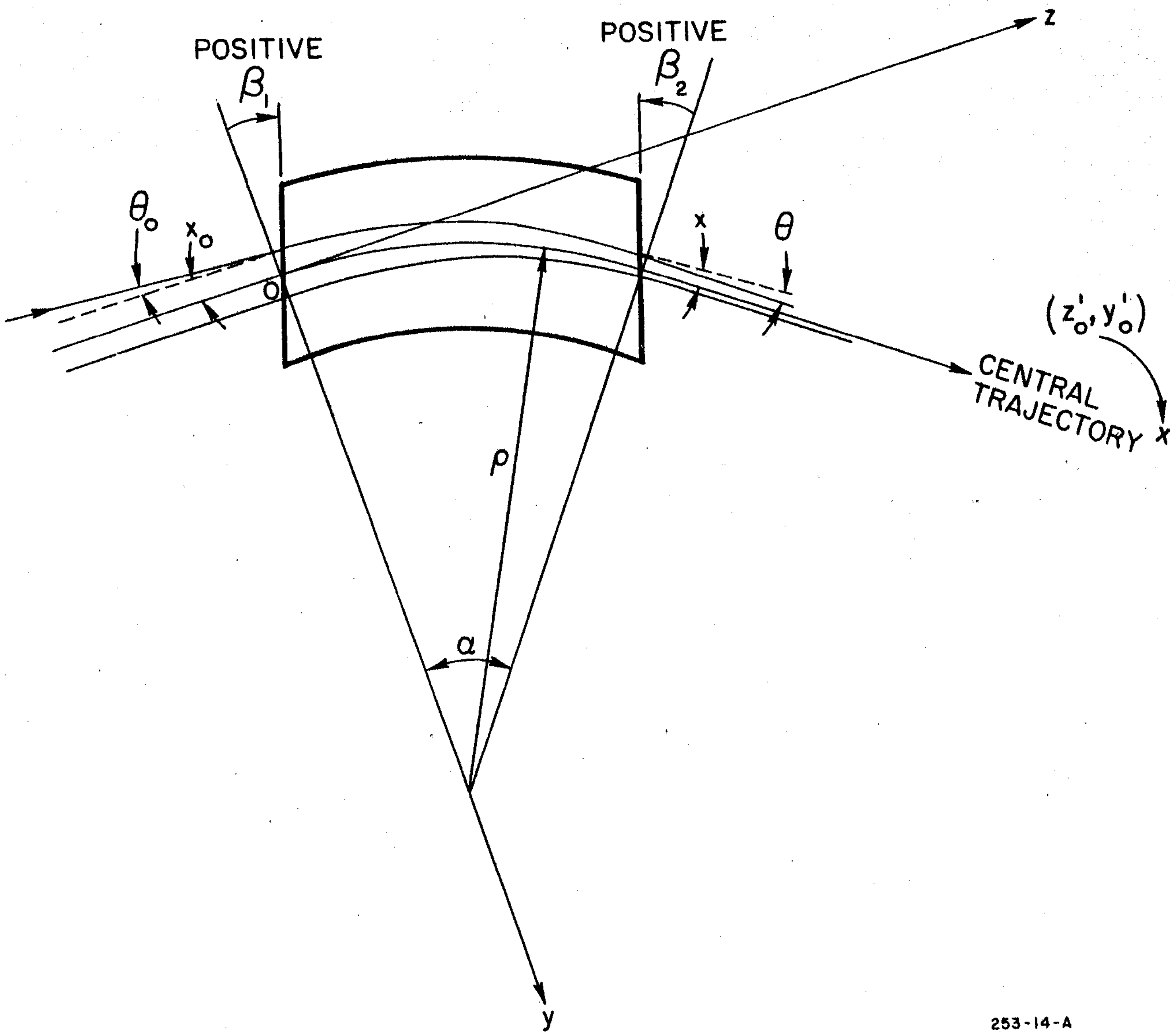

FIG. 14 - A COORDINATE SYSTEM FOR ANY DEFLECTING MAGNET

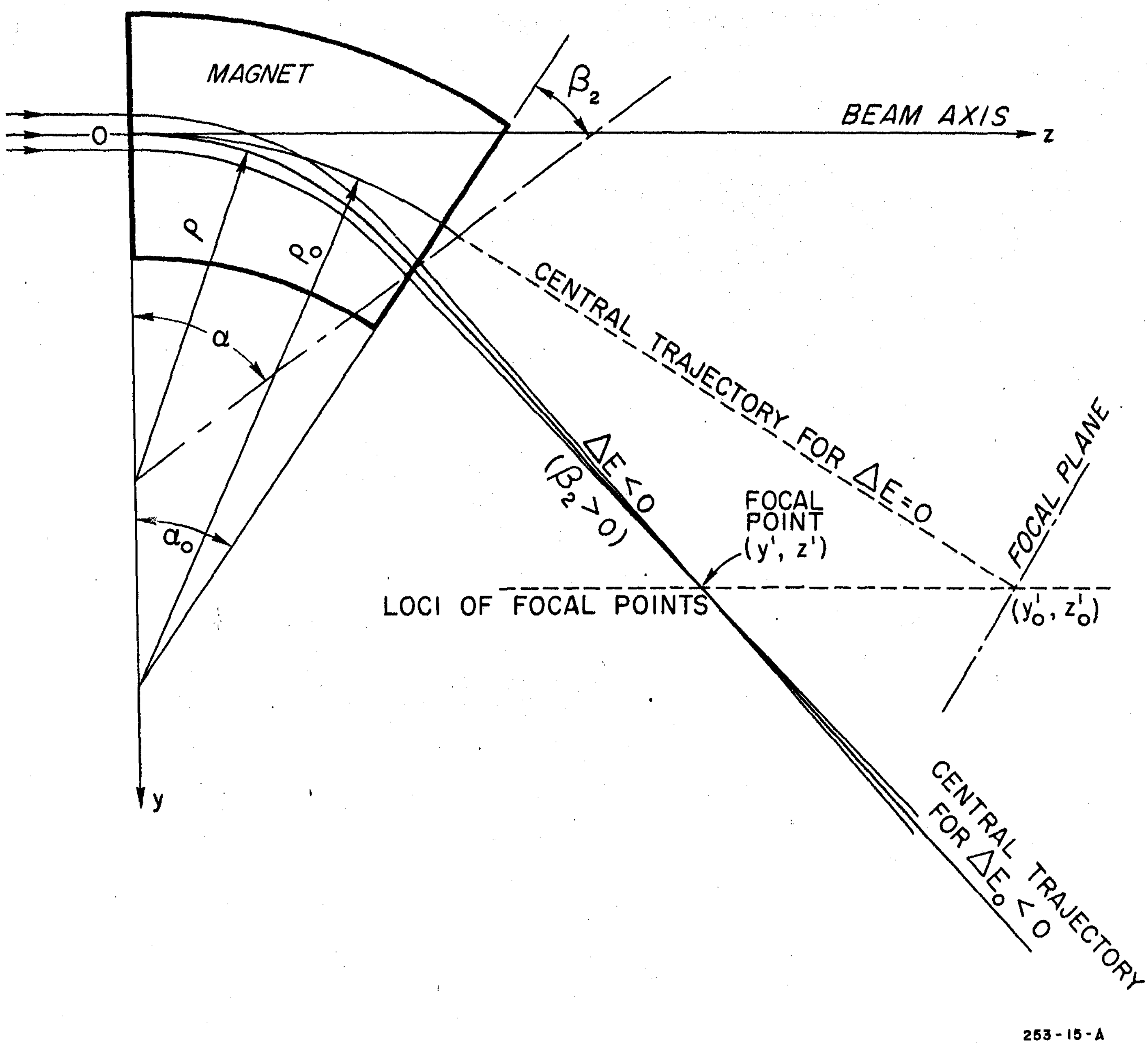

FIG. 15 - PARTICLE TRAJECTORY FOR $\Delta E < 0$, NORMAL INCIDENT CASE.

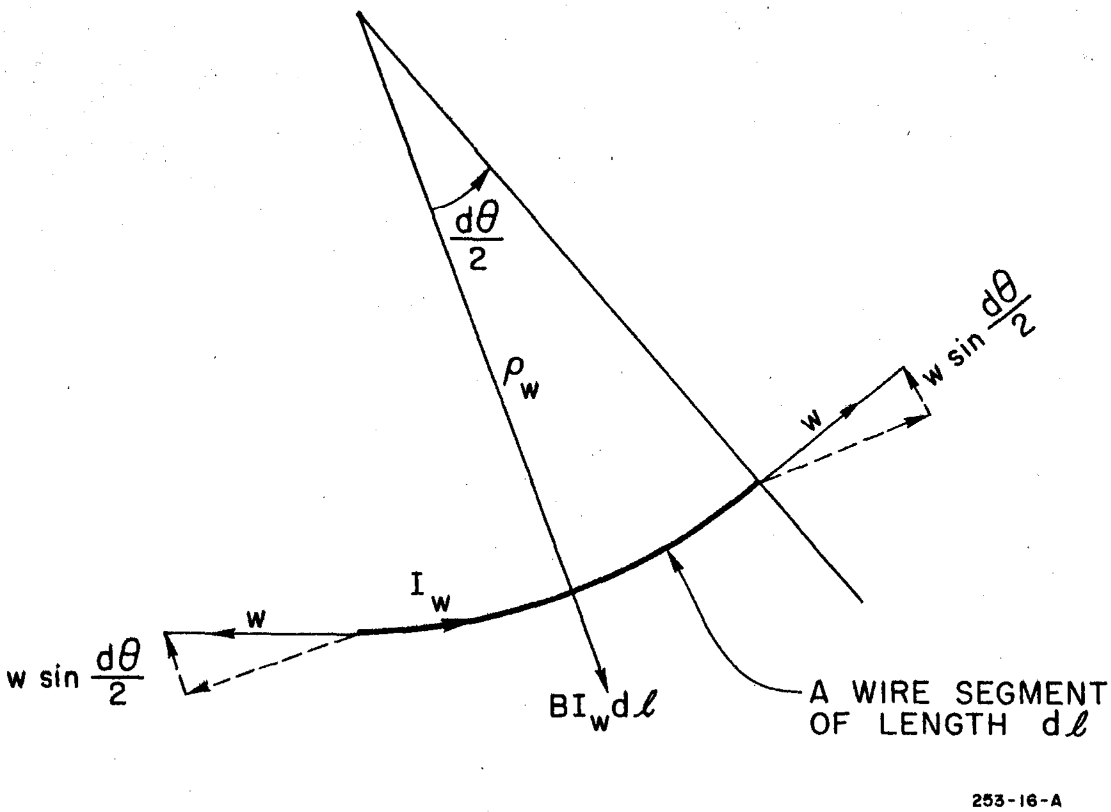

FIG. 16 - THE FORCES ACTING ON A SEGMENT OF A WIRE OF LENGTH $d\ell$, UNDER TENSION W IN A MAGNETIC FIELD B CARRYING A CURRENT I_w.